New Approach To Measure Protein Binding Based on a Parallel Artificial Membrane Assay and Human Serum Albumin

Elisabet Lázaro,[†] Philip J. Lowe,[‡] Xavier Briand,[§] and Bernard Faller*[,§]

Departament de Química Analítica, Universitat de Barcelona, Martí i Franquès 1, E-08028 Barcelona, Spain, Novartis Pharma AG, Modelling and Simulation, WSJ-27.1.22, CH-4002 Basel, Switzerland, and Novartis Institutes for BioMedical Research, WSJ-350.3.04, CH-4002 Basel, Switzerland

Received October 11, 2007

We report here a new, label-free approach to measure serum protein binding constants. The assay is able to measure HSA K_d values in the milli-molar to micromolar range. The protein is not immobilized on any surface and the assay self-corrects for nonspecific adsorption. No mass balance is required to get accurate binding constants and it is not necessary to wait for equilibrium to extract the binding constant. The assay runs in a 96-well format using commercially available parts and is, therefore, relatively easy to implement and automate. As the chemical membranes used are not water permeable, there is no volume change due to the osmotic pressure and pretreatment (soaking) is not necessary. The concept can potentially be extended to other proteins and could thus serve as a label-free technique for general binding constant measurements.

Introduction

Plasma protein binding is an important factor to understand the pharmacokinetics and pharmacodynamic properties of drug candidates, as it strongly influences drug distribution and determines the free fraction, which is available to the target. Human serum albumin (HSA[a]) is the most abundant plasma protein, so the determination of its binding constant (K_d) with early drug candidates is particularly relevant. In early drug discovery, protein binding is a key issue in compound optimization when compounds that are potent in a primary biochemical assay fail to retain activity in subsequent cell-based and in vivo assays. Other than pharmacokinetic clearance, two main reasons for this loss of activity are poor membrane permeability and high protein binding. This study shows that the measurement of passive permeability through an artificial membrane in the presence and absence of protein can be used to estimate the protein–ligand K_d and generate valuable information for compound optimization.

A broad variety of techniques have been applied to measure protein binding, with equilibrium dialysis and ultrafiltration being the most widely used methods.[1–3] Although attempts to increase the throughput with these methods are described in the literature,[4–6] they remain difficult to apply in early discovery. In addition, accurate rank ordering of compounds that are highly protein bound is a significant challenge, especially when recovery is not complete, and varies from compound to compound. Spectroscopic methods[7,8] are cheaper and faster alternatives that examine the molecular properties of the drug–protein complex; however, they do not correlate well with equilibrium dialysis for various reasons. More recently, some authors have proposed protein binding determinations using HSA immobilized on an HPLC stationary phase[9,10] or on beads.[11] However, these methods assume that the immobilized HSA retains its full binding characteristics and that nonspecific binding has little impact on the result.

In the method described in this paper, the protein-binding K_d value is estimated from transmembrane permeation kinetics measured in the presence and absence of protein.

Scheme 1. Chemical Equilibrium in the PAMPA-HSA Assay

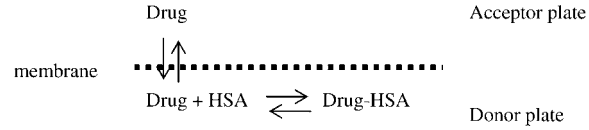

Assay Principle

A parallel artificial membrane permeation assay (PAMPA) is used to measure the permeation kinetics through an artificial membrane coated on a porous filter plate.[12–15] Various PAMPA assays have been described in the literature to measure passive (transcellular) permeability, with the aim to predict oral absorption of drug candidates. In this study, we report for the first time the use of a PAMPA to measure binding constants. Permeability is measured in the presence and absence of protein in the donor compartment, and the difference between the two experiments is used to estimate the binding constant. The key assumption in this approach is that only the free ligand is able to cross the membrane, while both the protein and the protein–ligand complex are either unable to cross the membrane, or do so at a velocity far lower than that of the free ligand (see Scheme 1).

The donor and acceptor compartments are separated by a thin liquid membrane coated on a porous filter in a 96-well microtiter-plate format (setup details available as Supporting Information). At the end of the incubation time, the compound concentration in the acceptor compartment is measured and then

* To whom correspondence should be addressed. Tel.: +41 61 324 7090. Fax: +41 61 324 3357. E-mail: bernard.faller@novartis.com.

[†] Universitat de Barcelona.

[‡] Novartis Pharma AG.

[§] Novartis Institutes for BioMedical Research.

[a] Abbreviations: A, surface of filterplate well × porosity; V_A, volume of acceptor well; V_D, volume of donor well; C_A, concentration in acceptor; C_D, concentration in donor; complex, HSA−ligand; K_h, membrane + non specificbinding sites distribution coefficient extracted from PAMPA kinetics; K_d, protein–ligand binding affinity (defined as k_{off}/k_{on}); k_{on}, association rate constant; k_{off}, dissociation rate constant; D_{mem}, membrane distribution coefficient measured by dual-phase potentiometric titration; D_{hxd}, hexadecane distribution measured by dual-phase potentiometric titration; V_M, apparent volume of the membrane (= membrane volume × D_{mem}); HSA, human serum albumin; P_a, apparent permeability; C_{ini}, initial concentration in donor; C_{eq}, theoretical concentration at equilibrium; C_M, concentration in the membrane.

10.1021/jm7012826 CCC: $40.75
Published on Web 03/19/2008

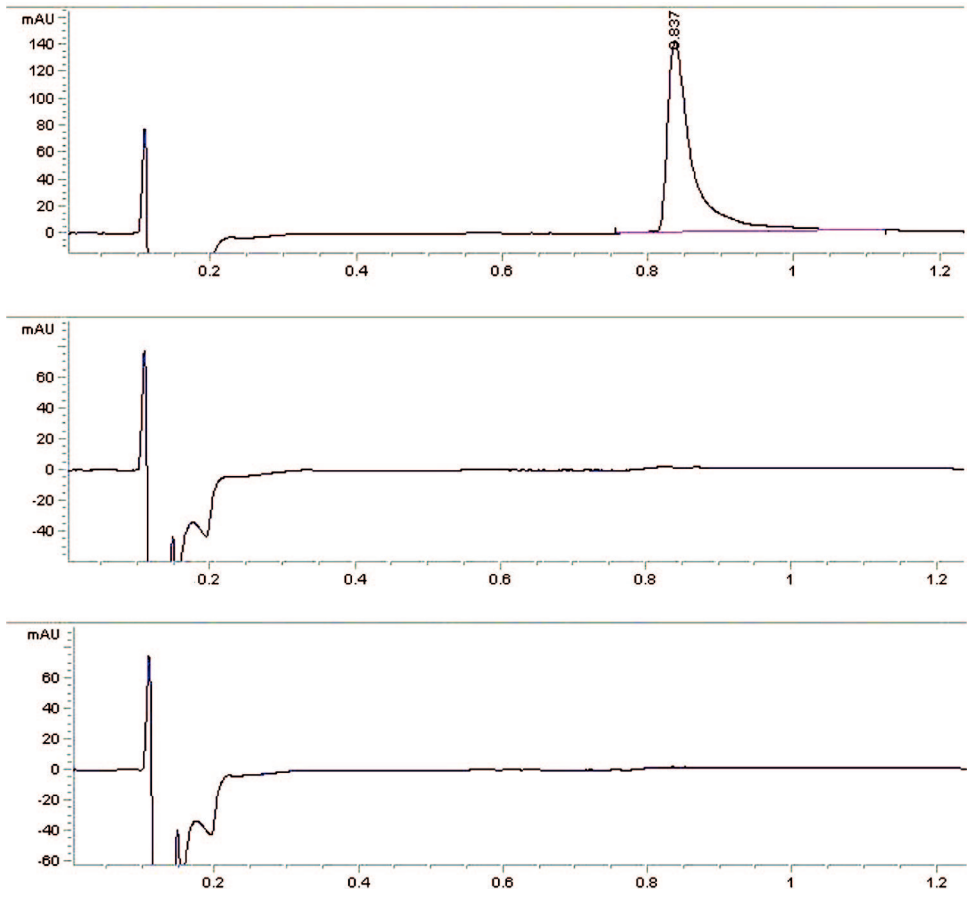

Figure 1. Permeability of HSA through the hexadecane and octanol membranes. Upper panel, 1 μM HSA (as a reference signal); Middle panel, donor and acceptor compartments separated by a hexadecane membrane. HPLC trace in acceptor compartment after 4 h incubation of 100 μM HSA in the donor compartment; Lower panel, donor and acceptor compartments separated by an octanol membrane. HPLC trace in acceptor compartment after 4 h incubation of 100 μM HSA in the donor compartment.

the apparent permeability (P_a) is calculated from the concentration vs. time data. In absence of protein, P_a can be calculated using the following differential equations, which describe passive diffusion under nonsink conditions:

$$\frac{dC_D}{dt} = -P_a A\left(\frac{C_D}{V_D} - \frac{C_A}{V_A}\right) \quad (1)$$

$$\frac{dC_A}{dt} = +P_a A\left(\frac{C_D}{V_D} - \frac{C_A}{V_A}\right) \quad (2)$$

where C_D, V_D, and C_A, V_A are the concentrations and volumes of the donor and acceptor compartment, respectively, and A is the accessible filter surface area (total filter area multiplied by the filter porosity factor).

Equation 3 is the solution of the above differential eqs 1 and 2:

$$P_a = -\frac{V_D V_A}{(V_D + V_A)At}\ln\left(1 - \frac{C_A}{C_{eq}}\right) \quad (3)$$

where

$$C_{eq} = \frac{V_D}{V_A + V_D}C_{ini} \quad (4)$$

C_{eq} is the theoretical concentration at equilibrium defined by 4 and C_{ini} is the initial concentration in donor plate ($t = 0$).

When HSA is added to the donor compartment, the apparent permeability (P_a) of the test compound decreases, because only the free fraction can diffuse through the membrane. The choice of the membrane material is critical for the assay. The ideal membrane is highly permeable to the free ligand but impermeable to the protein and ligand−protein complex. With HSA as the target protein, we found at least two chemical membranes fulfilling these criteria: hexadecane and octanol. HSA does not cross these membranes due to its low lipophilicity and high hydrogen bond potential (Figure 1). In the presence of protein, eq 1 becomes eq 5; new equations 6 and 7 are added to describe the formation and dissociation of the HSA−ligand complex. Equation 2 remains unchanged, as no protein is added to the acceptor compartment.

$$\frac{dC_D}{dt} = -P_a A\left(\frac{C_D}{V_D} - \frac{C_A}{V_A}\right) - k_{on}\,\mathrm{HSA}\cdot C_D + k_{off}\,\mathrm{Complex} \quad (5)$$

$$\frac{d\mathrm{HSA}}{dt} = -k_{on}\,\mathrm{HSA}\cdot C_D + k_{off}\,\mathrm{Complex} \quad (6)$$

$$\frac{d\mathrm{Complex}}{dt} = k_{on}\,\mathrm{HSA}\cdot C_D - k_{off}\,\mathrm{Complex} \quad (7)$$

All concentrations are expressed in molar units. Complex and HSA are the concentrations of protein–ligand complex and free HSA at time t, respectively.

Another phenomenon which potentially affects diffusion kinetics is membrane retention. Membrane retention is characterized by the membrane/buffer distribution coefficient, also known as the log D_{mem}. To take this phenomenon into account 5 becomes 8 and 2 becomes 9:

$$\frac{dC_D}{dt} = -P_a A\left(\frac{C_D}{V_D} - \frac{C_M}{V_M}\right) - k_{on}\mathrm{HSA}C_D + k_{off}\mathrm{Complex} \quad (8)$$

$$\frac{dC_A}{dt} = +P_a A\left(\frac{C_M}{V_M} - \frac{C_A}{V_A}\right) \quad (9)$$

where C_M is the concentration in the membrane compartment at time t and V_M is the apparent membrane volume, that is, membrane volume multiplied by the ligand distribution coefficient, K_h. In this paper, D_{mem} refers to the membrane distribution coefficient measured using an independent method (dual-phase potentiometric titration) and K_h is the membrane distribution coefficient derived from the PAMPA assay using equations 8 and 10. In the absence of nonspecific adsorption to the device, D_{mem} and K_h should be identical within the noise of the experiment. An additional equation that describes the concentration of the free ligand in the membrane is also needed (eq 10):

$$\frac{dC_M}{dt} = +P_a A\left(\frac{C_D}{V_D} - \frac{2C_M}{V_M} + \frac{C_A}{V_A}\right) \quad (10)$$

As there is no simple analytical solution to solve the differential equations 8 and 10, $C_A(t)$ was calculated using numerical integration with the Berkeley Madonna software.[16] Although the above equations decompose K_d into its microscopic constants ($K_d = k_{off}/k_{on}$), k_{off} was fixed at 1 s^{-1} in all data analyses. Berkeley Madonna is a differential equation solver developed by R. I. Macey and G. I. Oster at the University of California at Berkeley. It allows both simulation and fitting of one or more differential equations simultaneously.

Results

As recovery is a critical aspect in protein-binding measurement, especially with the lipophilic compounds encountered in modern drug discovery, we started to study the impact of nonspecific binding and membrane retention on the permeation kinetics. A simulation was carried out based on equations 8 and 10 using the Berkeley Madonna software. Figure 2 shows the theoretical concentration/time profiles obtained in the absence (Figure 2A) and presence of HSA (Figure 2B) in the donor compartment. Both HSA binding and membrane retention lead to a reduced concentration in the acceptor compartment and, thus, an underestimation of the true membrane permeability of the free test compound. Interestingly, the comparison between panel A and panel B shows that the shape of the concentration versus time curve is different. Membrane retention creates a lag phase, during which the membrane is filled with the ligand, before the compound effectively reaches the acceptor compartment (Figure 2A, curves C, D). This is not the case when the decrease in apparent permeability is caused by HSA binding (Figure 2B, curves C, D). This shows that recording appropriate time points allows one to (i) correct the apparent permeability for membrane retention and (ii) differentiate between protein binding and membrane trapping.

The impact of low k_{off} (and k_{on}) values on the permeability kinetics is shown in Figure 3. The assay has the capability to detect low microscopic rate constants if the association/dissociation process half-time is comparable or slower than the diffusion kinetics. When the microscopic rate constants are low ($k_{off} \leq 0.001$ s^{-1}), the diffusion of the free ligand through the membrane is faster than the binding to HSA (Figure 3, curves B, C) and, as a result, the concentration of the free ligand in the acceptor compartment goes down again due to slow binding of the free ligand to the protein in the donor compartment.

The model has been applied to 11 drugs with different properties in terms of lipophilicity (log $D_{7.4}$), polar surface area, acidic and basic character, with protein binding K_d data taken from literature sources.[7,8,17–46] Compound selection is shown in Table 1. The permeability of these 11 drugs (see chemical structures in Figure 4) was measured in the presence and absence of human serum albumin.

Figure 5 shows the concentration versus time profile of quinine, a low binding affinity compound[24] with a low membrane retention (log $D_{hxd} = -1.3$), in the absence (−) and presence of HSA (+) in the donor compartment. The solid lines are the best fit obtained with eqns 8−10 with log $P_a = -4.07$, log $K_h < 1$, and −log K_d (HSA) = 3.6.

Figure 6 shows the concentration versus time profile of warfarin, a high binding affinity compound[17–23] with low membrane retention (log $D_{hxd} = -2$) in the absence (−) and presence of protein in the donor compartment (+). The solid lines were obtained with log $P_a = -4.4$, log $K_h < 1$ and −log K_d (HSA) = 5.4. Comparison of Figures 5 and 6 shows that the impact of protein on the apparent permeability is much higher with warfarin than with quinine, consistent with its higher HSA binding affinity. Figure 7 shows chlorpromazine, a lipophilic compound (log $D_{hxd} = 2.6$) with a medium HSA binding affinity.[7,25,29–31] In this case, membrane retention significantly influences the $C_A(t)$, and the best fit was obtained with log $P_a = -2.5$, log $K_h = 3.4$, and −log K_d (HSA) = 4.3.

As described above, the method is based on the change in apparent permeability upon addition of protein to the donor compartment. One obvious limitation of this approach is with compounds that are poorly permeable through the membrane. Initially, the hexadecane membrane was designed to mimic transcellular gastrointestinal permeability,[13] and therefore, compounds with a poor transcellular permeability would be difficult to measure. This is typically the case of diflunisal, a peripherally active non-narcotic analgesic that diffuses poorly through the hexadecane membrane. Successful measurement of protein-binding K_d with the less lipophilic compounds was achieved by using an alternative membrane to separate free from protein-bound ligand. Octanol (5 μL of 30% octanol dissolved in hexane) was found to work well for most compounds with poor hexadecane permeability. Diflunisal (log $D_{oct} = 0.5$, log $D_{hxd} < -2$) was successfully measured using an octanol membrane. The HSA K_d does not depend on the nature of the membrane used to separate the free ligand from the HSA−ligand complex, as demonstrated with verapamil, which was measured using both hexadecane and octanol membranes. HSA −log K_d values of 3.2 and 3.5 were obtained using hexadecane and octanol, respectively. The difference between the two experiments is in the membrane retention, which is higher with the octanol membrane (log $K_h = 3.75$) compared with hexadecane (log $K_h = 2.1$).

The results obtained with the 11 test compounds are shown in Table 1, together with the HSA K_d values taken from literature sources. A very good agreement was found between the HSA K_d values obtained with the PAMPA−HSA assay and the reference values were taken from literature (Figure 8). Both sets agree with a correlation coefficient greater than 0.9 and a slope close to 1.

Most of the measurements in this study were performed with [HSA] = 100 μM and [ligand] = 50 μM. Data in Table 2

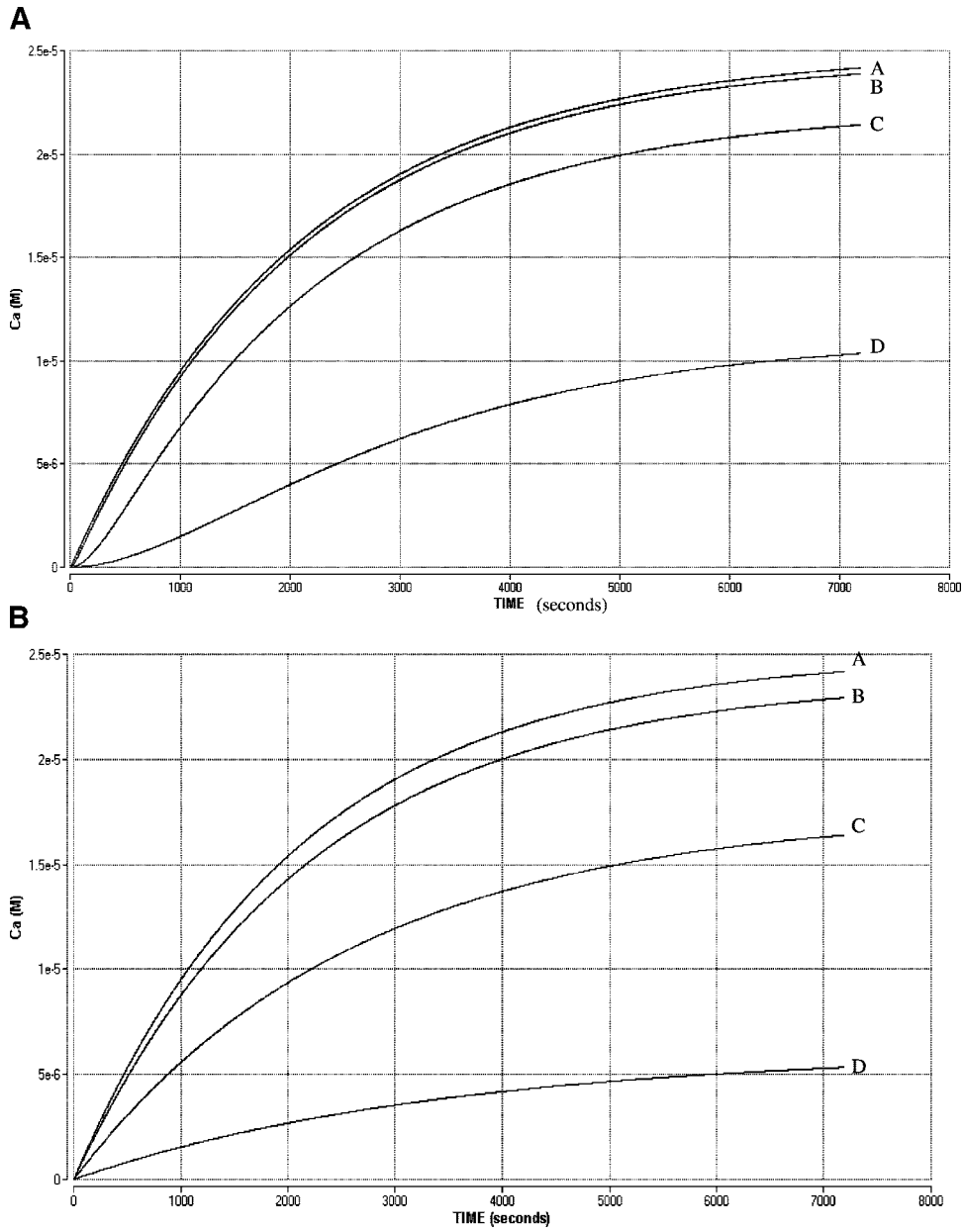

Figure 2. (A) Theoretical concentration/time profiles in the absence of HSA, obtained with log $P_a = -2.5$ and $D_{mem} = 1$, 10, 100, and 1000 (A−D). The loading concentration is 50 μM, $V_A = 0.3$ mL, $V_D = 0.3$ mL, and the membrane volume is 0.75 μL. (B) Theoretical concentration/time profiles in the presence of HSA, obtained with log $P_a = -2.5$, log $D_{mem} = 1$, and HSA $K_d = 10^{-1}$, 10^{-3}, 10^{-4}, and 10^{-5} M (A−D). The loading concentration is 50 μM, $V_A = 0.3$ mL, $V_D = 0.3$ mL, and the membrane volume is 0.75 μL.

demonstrate the reproducibility of the method with different drug/protein concentrations.

Discussion

Careful inspection of Figures 5 and 6 shows that there is a small lag phase in the $C_A(t)$ kinetics. This cannot be explained by membrane retention as the membrane (hexadecane) distribution coefficients of quinine and warfarin are too small (−1.3 and −2, respectively). What likely explains this deviation from linearity is nonspecific adsorption of the compounds in the acceptor compartment. The compounds only appear after the nonspecific binding sites are fully saturated, but the K_h parameter in equations 8−10 does not differentiate between membrane retention and nonspecific binding in the acceptor compartment. For this reason, the log K_h values are always equal or higher than the membrane distribution coefficients log D_{mem} measured independently. When membrane retention becomes significant, as with chlorpromazine, the relative contribution of nonspecific binding is lower and, in this case, log K_h becomes close to log D_{mem} (3.4 vs 2.6 for chlorpromazine).

The method presented here has the advantage of being label-free and does not require immobilization of the protein on a surface, which can potentially affect the binding affinity. Desipramine can be used to illustrate this point; a $-\log K_d$ of 4.85 has been reported using a fluorescent method,[25] while a quite different value ($-\log K_d = 3.48$) has been recently reported using an ultrafiltration technique.[26] Interestingly, using the PAMPA−HSA method gives a result that is in good agreement with the one obtained by ultrafiltration (3.10 vs 3.48).

We have shown that the assay dynamic range is about 3 log units from millimolar (desipramine, $-\log K_d = 3.5$) down to micromolar (diflunisal, $-\log K_d = 6.2$). This window can be further adjusted to the desired range depending on the protein and ligand concentrations used.

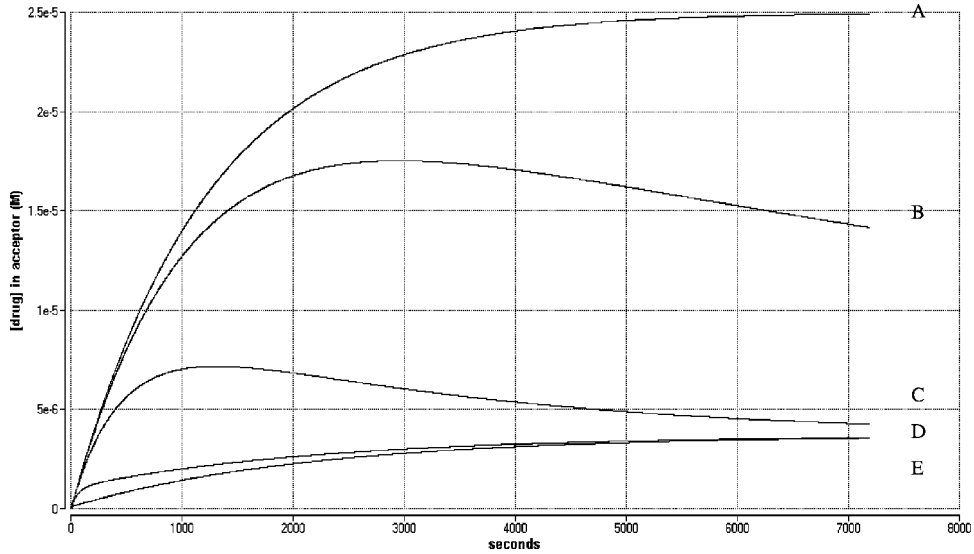

Figure 3. Impact of slow dissociation (low k_{off}) on the concentration in acceptor time profile. Eqns 8−10 were used to simulate the impact of low on and off rates on Ca(t). Conditions were $K_d = 5\ \mu$M, [drug] = 50 μM, HSA = 100 μM. Curves were calculated for $k_{off} = 0.00001$, 0.0001, 0.001, and 0.01 s^{-1} (curves B, C, D, and E, respectively). The reaction is initiated by the addition of the drug to the PAMPA sandwich containing HSA in the donor compartment at time 0. Curve A represents Ca(t) in the absence of protein in the donor compartment.

Table 1. Result Summary of PAMPA-HSA Results Obtained with the 11 Test Compounds[a]

compound	A/B	ClogP	membrane	log P_a	log K_h	PAMPA−HSA −log K_d	−log K_d (lit. value)	avg ref value used[i]
chlorpromazine[7,25,29–31]	B	5.3	Hxd	−2.51	3.4	4.26 (91.5)	4.62[c], 3.89[b], 4.25[b]	4.26
desipramine[26]	B	4.5	Hxd	−3.01	1.3	3.07 (41.3)	3.48[d]	3.48
diazepam[8,18–20,32–37]	B	3.0	Hxd	−2.87	1.6	4.61 (96.0)	5.0[b], 4.89[b], 3.94[g]	4.60
diclofenac[27,38]	A	4.7	Hxd	−4.71	<1	5.61 (99.6)	5.74[b], 5.70[b]	5.72
diflunisal[27,28]	A	4.4	Hxd	−6.10	<1	undefined	5.70[b], 6.70[b]	6.20
diflunisal[27,28]	A	4.4	Oct	−2.82	1.4	5.91 (99.8)	5.70[b], 6.70[b]	6.20
oxazepam[39]	B	2.3	Hxd	−4.09	<1	4.16 (89.6)	4.55[c]	4.55
propranolol[40]	B	2.7	Hxd	−4.00	1.8	3.36 (57.8)	3.58[b]	3.58
quinine[24]	B	2.8	Hxd	−4.07	<1	3.51 (65.8)	3.88[d]	3.88
tolbutamide[41–45]	A	2.5	Hxd	−4.96	<1	5.22 (99.0)	4.61[b], 4.68[h], 4.90[f]	4.73
verapamil[46]	B	4.5	Hxd	−2.85	2.09	3.19 (48.3)	3.43[e]	3.43
verapamil[46]	B	4.5	Oct	−2.73	3.75	3.53 (66.9)	3.43[e]	3.43
warfarin[17–23]	A	2.9	Hxd	−4.40	<1	5.33 (99.2)	5.23[b], 5.20[d], 5.48[f]	5.30
warfarin[17–23]	A	2.9	Oct	−3.86	<1	5.37 (99.3)	5.23[b], 5.20[d], 5.48[f]	5.30

[a] A, acids; B, bases. All measurements have been performed at pH 7.4. The numbers in brackets represent the fraction bound in % derived from the K_d values assuming a [HSA] = 600 μM and [drug] = 5 μM. ClogP values were obtained with the BioByte software v. 4.71. [b] Equilibrium dialysis. [c] Spectroscopic technique. [d] Ultrafiltration. [e] Capillary electrophoresis. [f] HPLC chromatography. [g] Gel filtration. [h] Calorimetry. [i] Average value used to compare with PAMPA−HSA values (Figure 7).

There are also some limitations in this approach that we would like to briefly discuss. The first one is that not all compounds can be measured with the same chemical membrane; We have shown that general lipophilic compounds can be measured with a hexadecane membrane, whereas more hydrophilic compounds (like Diflunisal) only worked with an octanol membrane. Can one select the appropriate membrane prior to the experiment? As a rule, we would propose that compounds with calculated octanol/water log D values lower than 1 will not work with the hexadecane membrane; however, there are probably a few exceptions to that rule. The other option is to run the assay with both membranes in parallel and select the relevant one after the experiment.

Another aspect that deserves some comments lies with the fact that the compounds in the training set are "old" drugs and, therefore, how well will the method work with "real life" discovery compounds? Drug candidates are generally more difficult to handle than generic drugs in many assays, essentially because they are often more lipophilic, bigger, and less-soluble. To answer the question whether the method would be able to cope with these more difficult compounds, experiments were done at a lower ligand concentration with propranolol (Table 2). Essentially, the log K_d values obtained at 10 μM was identical to the one obtained at 50 μM. Extremely insoluble compounds might require to go further down in ligand concentration, and the lower limit of quantification of the analytical method can then become rate limiting. However, the same limitation applies to all known methods, as LC-MS/MS is the readout of choice in most if not all high-quality protein-binding assays. High lipophilicity is another characteristics of new "real life" compounds and leads to membrane retention and nonspecific binding. We have shown that this is usually not an issue with the method presented here, as these phenomena are taken into account in the K_h parameter.

A common issue encountered with protein-binding assays is the resolution, which can be reliably obtained for highly protein-bound compounds. To get a feel for the performance of our method, we repeated experiments over a six-week time period with a number of highly protein-bound compounds (Table 3).

In general, the resolution of the method depends on the targeted K_d value and the concentration of HSA and ligand used. In this study, most measurements were done at 100 μM HSA with the intend to cover a K_d from the millimolar to the micromolar range. We suggest to use these conditions as a first

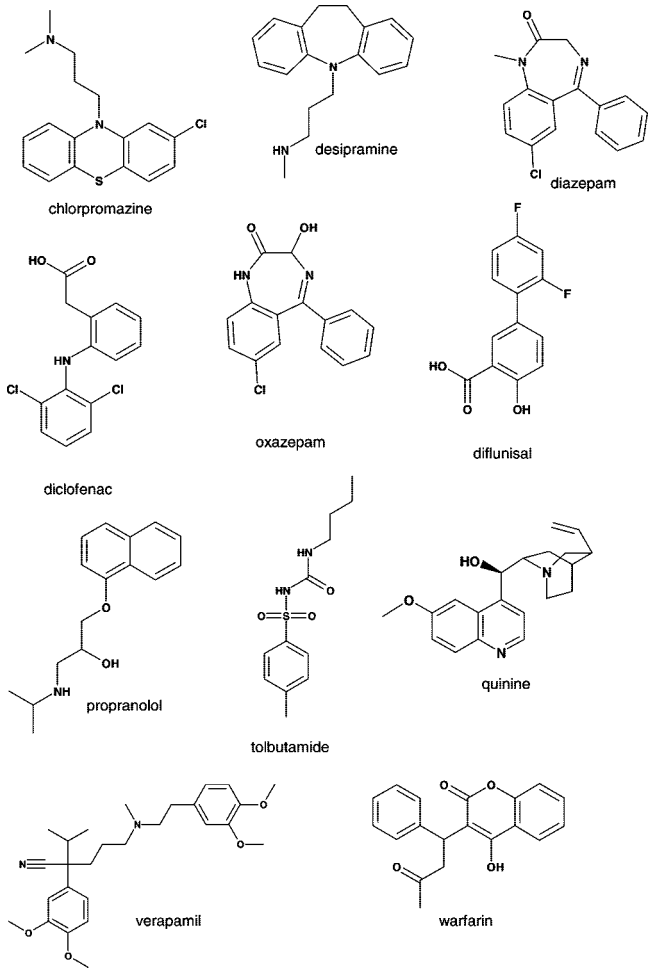

Figure 4. Chemical structures of the compounds of the test set.

line generic screen. For refined measurements, one can repeat the experiment with lower HSA concentration for very strong binders (permeability in the presence of protein drops below the lowest limit of quantification) or with a higher HSA concentration for weak binders (permeability ± protein becomes too small).

In comparison with membrane dialysis, the analytical burden is more or less identical, as both methods used LC-MS/MS as a readout. The advantages of the PAMPA−HSA approach are elsewhere; this approach is faster (i) with no need to reach equilibrium to estimate the binding constant (and lower risk of compound or protein degradation), and (ii) the loss of material to the plate walls or the membrane interface does not affect the quality of the result. As with alternative approaches, membrane retention and nonspecific binding to the walls of the device does occur, but it is taken care in the analysis of the kinetic data as the K_h parameter accounts for compound retention. In principle, the kinetic approach described here can also be used with an equilibrium dialysis technique and would be a powerful alternative to mass balance calculations. However, there are a few advantages provided by the liquid membranes. Liquid membranes allow equilibrium to be reached faster because the effective surface of exchange provided by a liquid membrane is larger. As these membranes are not permeable to water, there is no volume change due the osmotic pressure (and, therefore, no correction needed). Finally, there is no need to pretreat membranes prior to use, which makes it easier for automation. The PAMPA−HSA approach can also be viewed as a direct way to study the impact of protein binding on drug absorption or diffusion through cell membranes. In this respect, the hexadecane membrane gives the ability to establish and maintain a pH gradient between the donor and the acceptor compartment, which would not be possible with the traditional membrane dialysis technique.

Perhaps a more general application of this work lies in the use of permeability kinetics as opposed to end point measurements as a method to correct permeability values for adsorption, such as nonspecific binding and membrane trapping. For example, in cell-based permeability assays (Caco-2, MDCK), poor compound recovery has been identified as a factor that should be taken into account when judging the validity of the result. We have shown that permeability corrected from nonspecific binding can be estimated from the permeability time course. This could be a powerful alternative to the traditional recovery calculations (mass balance) performed in cell-based permeability and PAMPA assays.

The assay principle described in this study could also be considered as a general label free technology to study protein–

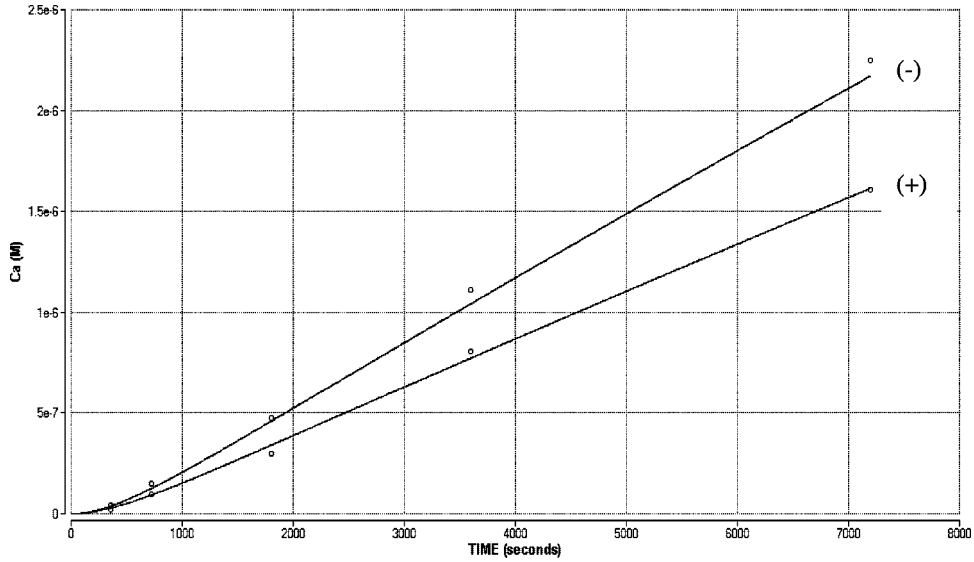

Figure 5. Concentration in acceptor (C_A) vs time profile of quinine in presence (+) and absence of HSA (−) in the donor compartment. Open circles represent the measured concentrations in acceptor compartment and the solid line is the best fit obtained using eqns 8−10.

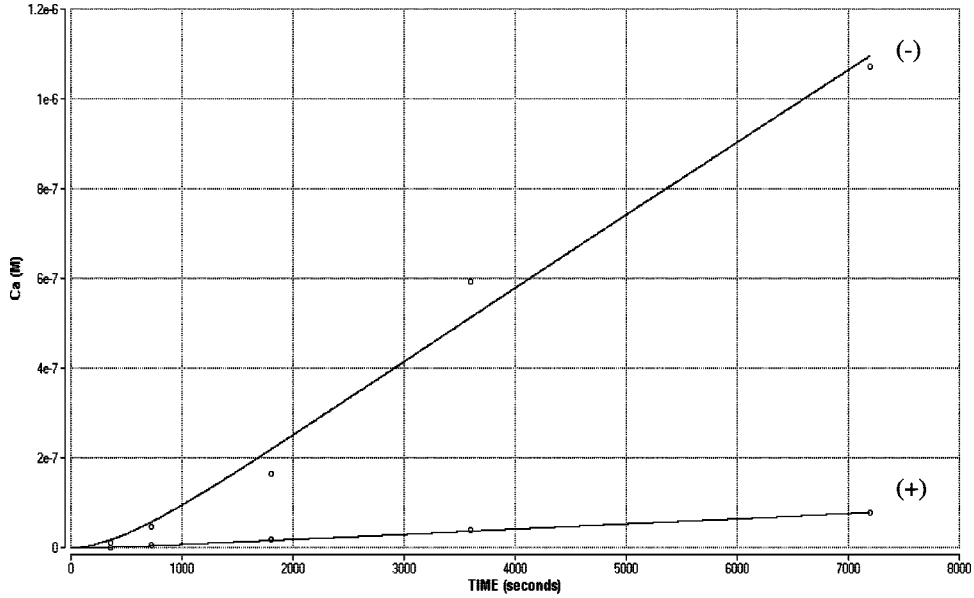

Figure 6. Concentration in acceptor (C_A) vs time profile of warfarin in presence (+) and absence (−) of HSA in the donor compartment. Open circles represent the measured concentrations in acceptor compartment and the solid line is the best fit obtained using eqns 8−10.

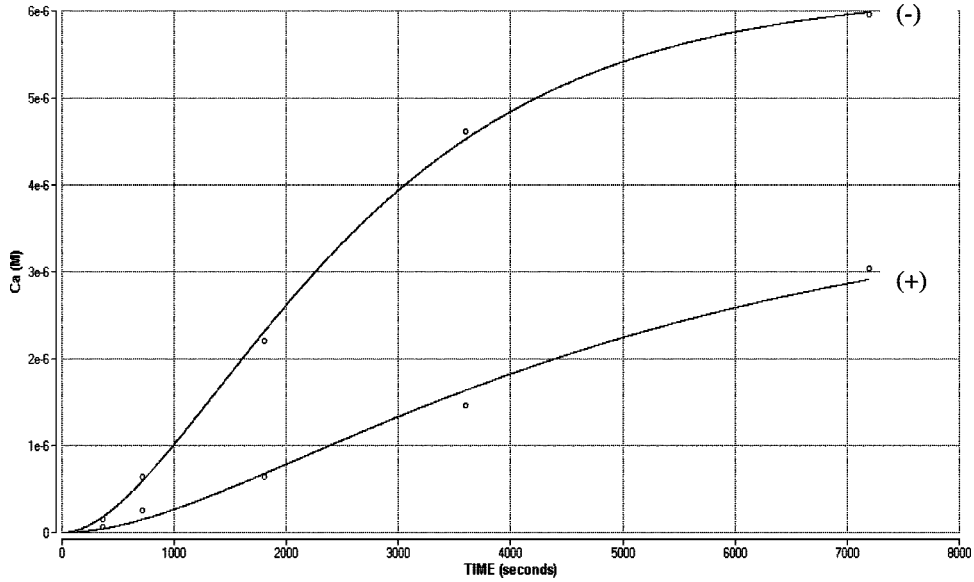

Figure 7. Concentration in acceptor (C_A) vs time profile of chlorpromazine in presence (+) and absence of HSA (−) in the donor compartment. Open circles represent the measured concentrations in acceptor compartment and the solid line is the best fit obtained using eqns 8−10.

ligand interactions. In particular, water-soluble proteins are expected to behave similarly to HSA and a chemical liquid membrane, such as those described in this study, will most probably separate most free ligands from the protein–ligand complexes efficiently.

Experimental Section

Reagents. All drugs were purchased from Sigma (Div. of Fluka Chemie AG, Buchs, Switzerland) and were dissolved in dimethyl sulfoxide (DMSO) at a concentration of 10 mM each and used without further purification. DMSO and hexane were obtained from Merck KGaA (Darmstadt, Germany) with a purity grade >99.8% and >99%, respectively. Hexadecane (>98%) and 1-octanol (99.5%) were purchased from Fluka and Riedel-de Haen, respectively (both from Sigma-Aldrich Chemie GmbH, Buchs, Switzerland). Human serum albumin (HSA), 99% fatty acid free, essentially globulin-free, was from Sigma. Phosphate buffer, pH 7.4 (0.014 M KH_2PO_4 and 0.054 M Na_2HPO_4), was from Fluka.

Analytics. The LC-MS/MS analyses were performed with a system equipped with two Rheos pumps 2000 (Flux Instruments, Basel, Switzerland) and a TSQ Quantum Discovery Max detector equipped with an electrospray ionization (ESI) source (ThermoFinnigan, San Jose, CA, U.S.A.). Nitrogen is used as a nebulizer gas at 40 psi, while the auxiliary gas is set at 10 psi. The capillary voltage is set at 4 kV, and its temperature is set at 350 °C. The collision pressure is 1 mTorr. The 96-well plates containing the samples are stored at 20 °C. Prior to injecting the sample, a solution of ACN/water 1/1 with internal standards (1.0 μM alprenolol for positive mode and 1 μM warfarin for negative mode) is added to the sample. The mobile phase is composed of a mixture of acetonitrile and water (containing 0.1% (v/v) of formic acid). Samples are injected (20 μL in a loop of 10 μL) and chromatographed on a Zorbax SB-C18, 30 × 2.1 mm, 1.8μm, column (Millian SA, Meyrin/Geneva, Switzerland) at a flow rate of 0.25 mL/min using to the following gradient: 0−1 min constant mobile phase composition of 5% acetonitrile; 1−3 min linear gradient from 5 to 100% acetonitrile; 3−4.8 min remained constant; 4.8−4.81

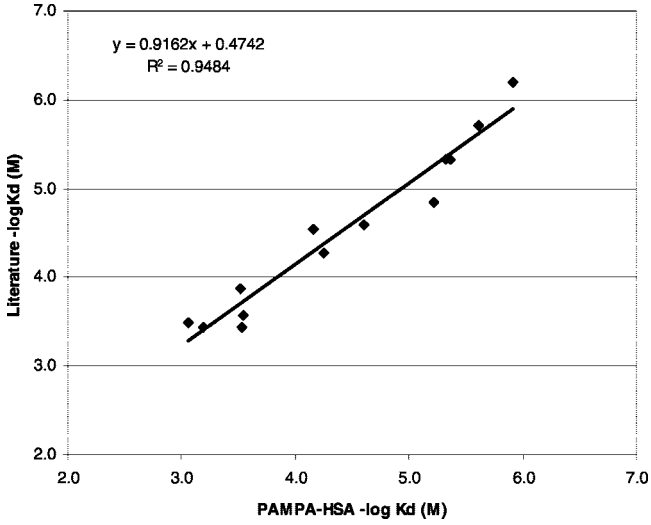

Figure 8. Correlation between literature and PAMPA−HSA K_d values.

Table 2. Impact of Drug and Protein Concentrations on K_d Determination

[propranolol], μM	[HSA], μM	log P_a	log K_h	PAMPA −log K_d
10	50	−4.2	1.3	3.45
10	100	−4.2	1.5	3.18
10	300	−4.0	1.8	3.22
10	600	−4.0	2.0	3.20
50	100	−4.0	1.8	3.36

Table 3. Assay Variability for Highly Protein-Bound Compounds[a]

	$N = 1$	$N = 2$	$N = 3$
warfarin	5.24 (99.0)	5.39 (99.3)	5.33 (99.2)
tolbutamide	5.56 (99.5)	4.95 (98.2)	5.16 (98.9)
diclofenac	5.61 (99.6)	5.60 (99.6).	5.61 (99.6)
diazepam	4.48 (94.7)	4.64 (96.3)	4.70 (96.7)
chlorpromazine	4.22 (90.8)	4.03 (86.5)	4.52 (95.2)

[a] Numbers are the PAMPA−HSA log $1/K_d$ (M) obtained from three independent experiments performed over a six-week time period using [HSA] = 50 μM and [ligand] = 100 μM. The numbers in brackets represent the fraction bound in % derived from the K_d values, assuming a [HSA] = 600 μM and [drug] = 5 μM.

linear gradient back to 5% acetonitrile; and 4.81−6 min was constant. The use of two chromatographic pumps allowed the MS analysis of one column elute while the other column is reconditioned, reducing therefore the total run time per sample to 4.8 min.

Permeability Measurements. Permeation experiments are carried out in a teflon 96-well plate, which acts as the donor compartment. All wells are filled with 300 μL of 50 μM drug solution in buffer pH = 7.4, containing 0.75% DMSO, and a little magnet is placed in each one. Half of the plate contains 100 μM HSA and the other half is protein-free. Microtiter filter plates obtained from Millipore AG (Zug, Switzerland) are used as acceptor plates. Each well of the filter plate is impregnated with 5 μL of a 15% (v/v) hexadecane solution (or 5 μL of a 30% (v/v) octanol solution) dissolved in hexane and incubated for 15 min until complete evaporation of hexane. After that, the acceptor compartment is hydrated with 300 μL of phosphate buffer, pH = 7.4. The resulting sandwich construct (acceptor plate above donor plate) is incubated at room temperature under constant stirring. At different time points (0.1, 0.2, 0.5, 1 and 2 h), 75 μL from acceptor plate wells is transferred to a disposable polystyrene plate and loaded to the LC-MS autosampler. Each sample is quantified by comparing the peak surface area of the analyte with a 25 μM (theoretical equilibrium concentration) reference solution prepared independently.

To ensure that the donor/acceptor fluxes are not due to porous or unstable hexadecane layers, the stability of the membranes is tested by electrical resistance measurements at the end of the 2 h incubation. These measurements are performed using a Keithley 6517A electrometer (Keithley Instruments S.A., Dübendorf, Switzerland) with Ag/AgCl electrodes from World Precision Instruments (Berlin, Germany). Trans-wells with electrical resistance lower than 25 kOhm are discarded.

Measurement of HSA Permeability. HSA is quantified using an LC-UV method. Analyses were performed with an Agilent 1200 series LC-UV HPLC with a binary pump and a diode array detector (Agilent Technologies, Waldbronn, Germany). The chromatography was performed on a Vydac 214TP C4 column, 50 × 2.1 mm, 5 μm (Bucher Biotec AG, Basel, Switzerland), maintained at 40 °C. The mobile phase solution is composed of acetonitrile and water delivered at 1.75 mL/min. Trifluoroacetic acid (TFA, 0.1%) is added in the mobile phase as an ion pair agent. The initial condition is 37% acetonitrile during 0.59 min; 0.59−0.6 min linear gradient from 37 to 40% acetonitrile; 0.6−1.0 min remained constant; 1.0−1.1 min linear gradient back to 37%; and is then constant until 2 min. The analytical wavelength was set at 210 nm.

Acknowledgment. E.L. was supported by a grant from the Spanish Government (AP2002-3049). We also thank Dr. Markus Weiss (Novartis Pharma AG) for helpful discussions and for providing reference data.

Supporting Information Available: Berkeley Madonna script used to solve eqns 8−10, and technical details of the PAMPA sandwich. This information is available free of charge via the Internet at http://pubs.acs.org.

References

(1) Kurz, H.; Trunk, H.; Weitz, B. Evaluation of methods to determine protein-binding of drugs. Equilibrium dialysis, ultrafiltration, ultracentrifugation, gel filtration. *Arzneim.-Forsch.* **1977**, *27*, 1373–1380.
(2) Bowers, W. F.; Fulton, S.; Thompson, J. Ultrafiltration vs equilibrium dialysis for determination of free fraction. *Clin. Pharmacokinet.* **1984**, *9*, 49–60.
(3) Sebille, B.; Zini, R.; Madjar, C. V.; Thuaud, N.; Tillement, J. P. Separation procedures used to reveal and follow drug-protein binding. *J. Chromatogr., A* **1990**, *531*, 51–77.
(4) Fung, E. N.; Chen, Y.; Lau, Y. Y. Semi-automatic high-throughput determination of plasma protein binding using a 96-well plate filtrate assembly and fast liquid chromatography-tandem mass spectrometry. *J. Chromatogr., B* **2003**, *795*, 187–194.
(5) Wan, H.; Rehngren, M. High-throughput screening of protein binding by equilibrium dialysis combined with liquid chromatography and mass spectrometry. *J. Chromatogr., A* **2006**, *1102*, 125–134.
(6) Banker, M: J.; Clark, T. H.; Williams, J. A. Development and validation of a 96-well equilibrium dialysis apparatus for measuring plasma protein binding. *J. Pharm. Sci.* **2003**, *92* (5), 967–974.
(7) Gabay, S.; Huang, P. C. The binding behavior of phenothiazines and structurally related compounds to albumin from several species. *Adv. Biochem. Psychopharmacol.* **1974**, *9*, 175–189.
(8) Brodersen, R.; Sjodin, T.; Sjoholm, I. Independent binding of ligands to human serum albumin. *J. Biol. Chem.* **1977**, *252*, 5067–5072.
(9) Valko, K.; Nunhuck, S.; Bevan, C.; Abraham, M. H.; Reynolds, D. P. Fast gradient HPLC method to determine compounds binding to human serum albumin. Relationships with octanol/water and immobilized artificial membrane lipophilicity. *J. Pharm. Sci.* **2003**, *92*, 2236–2248.
(10) Hollosy, F.; Valko, K.; Hersey, A.; Nunhuck, S.; Keri, G.; Bevan, C. Estimation of volume of distribution in humans from high throughput HPLC-based measurements of human serum albumin binding and immobilized artificial membrane partitioning. *J. Med. Chem.* **2006**, *49*, 6958–6971.
(11) Hartmann, T.; Schmitt, J.; Rohring, C.; Nimptsch, D.; Noller, J.; Mohr, C. ADME related profiling in 96 and 384 well plate format−A novel and robust HT-assay for the determination of lipophilicity and serum albumin binding. *Curr. Drug Delivery* **2006**, *3*, 181–192.
(12) Kansy, M.; Senner, F.; Gubernator, K. Physicochemical high throughput screening: Parallel artificial membrane permeation assay in the description of passive absorption processes. *J. Med. Chem.* **1998**, *41* (7), 1007–1010.
(13) Wohnsland, F.; Faller, B. High-throughput permeability pH profile and high-throughput alkane/water log *P* with artificial membranes. *J. Med. Chem.* **2001**, *44*, 923–930.

(14) Sugano, K.; Nabuchi, Y.; Machida, M.; Aso, Y. Prediction of human intestinal permeability using artificial membrane permeability. *Int. J. Pharm.* **2003**, *257* (1–2), 245–251.
(15) Avdeef, A.; Bendels, S.; Di, L.; Faller, B.; Kansy, M.; Sugano, K.; Yamauchi, Y. Parallel artificial membrane permeability assay (PAMPA)-critical factors for better predictions of absorption. *J. Pharm. Sci.* **2007 96**, (11), 2893–2909.
(16) Berkeley Madonna, http://www.berkeleymadonna.com/, http://www.berkeleymadonna.com/BM%20User's%20Guide%208.0.pdf,accessed 31-Aug-2007.
(17) Zaton, A. M.; Ferrer, J. M.; Ruiz de Gordoa, J. C.; Marquinez, M. A. Binding of coumarins to site I of human serum albumin. Effect of the fatty acids. *Chem.-Biol. Interact.* **1995**, *97*, 169–174.
(18) Kragh-Hansen, U. Evidence for a large and flexible region of human serum albumin possessing high affinity binding sites for salicylate, warfarin, and other ligands. *Mol. Pharmacol.* **1988**, *34*, 160–171.
(19) Kragh-Hansen, U. Relations between high-affinity binding sites of markers for binding regions on human serum albumin. *Biochem. J.* **1985**, *225*, 629–638.
(20) Vestberg, K.; Galliano, M.; Minchiotti, L.; Kragh-Hansen, U. High-affinity binding of warfarin, salicylate and diazepam to natural mutants of human serum albumin modified in the C-terminal end. *Biochem. Pharmacol.* **1992**, *44*, 1515–1521.
(21) Sengupta, A.; Hage, D. S. Characterization of minor site probes for human serum albumin by high-performance affinity chromatography. *Anal. Chem.* **1999**, *71*, 3821–3827.
(22) Brown, K. F.; Crooks, M. J. Displacement of tolbutamide, glibencalmide, and chlorpropamide from serum albumin by anionic drugs. *Biochem. Pharmacol.* **1976**, *25*, 1175–1178.
(23) Chattopadhyay, A.; Tian, T.; Kortum, L.; Hage, D. S. Development of tryptophan-modified human serum albumin columns for site-specific studies of drug-protein interactions by high-performance affinity chromatography. *J. Chromatogr., B: Biomed. Sci. Appl.* **1998**, *715*, 183–190.
(24) Paubel, J. P.; Niviere, P. La liaison des molécules organiques thérapeutiques avec les protéines: Cas de la quinine. *Eur. J. Med. Chem.* **1974**, *9*, 508–512.
(25) Sharples, D. Competition for plasma protein binding sites between phenothiazine tranquilizers and iminodibenzyl antidepressants. *J. Pharm. Pharmacol.* **1975**, *27*, 379–381.
(26) Szymura-Oleksiak, J.; Wyska, E.; Wasieczko, A. Pharmacokinetic interaction between imipramine and carbamazepine in patients with major depression. *Psychopharmacology (Berlin)* **2001**, *154*, 38–42.
(27) Honore, B.; Brodersen, R. Albumin binding of anti-inflammatory drugs. Utility of a site-oriented versus a stoichiometric analysis. *Mol. Pharmacol.* **1984**, *25*, 137–150.
(28) Larsen, C. G.; Larsen, F. G.; Jakobsen, P.; Brodersen, R. Multiple cobinding of two ligands to serum albumin: a stoichiometric description of binding equilibria. *Arch. Biochem. Biophys.* **1985**, *239*, 74–86.
(29) Huang, P. C.; Gabay, S. Examination of phenothiazine-albumin interaction by ultraviolet difference spectrophotometry. *Biochem. Pharmacol.* **1974**, *23*, 957–972.
(30) Nambu, N.; Nagai, T. Binding of phenothiazines to bovine serum albumin and related phenomena. *Chem. Pharm. Bull. (Tokyo)* **1972**, *20*, 2463–2470.
(31) Romer, J.; Bickel, M. H. A method to estimate binding constants at variable protein concentrations. *J. Pharm. Pharmacol.* **1979**, *31*, 7–11.
(32) Bagatolli, L. A.; Kivatinitz, S. C.; Fidelio, G. D. Interaction of small ligands with human serum albumin IIIA subdomain. How to determine the affinity constant using an easy steady state fluorescent method. *J. Pharm. Sci.* **1996**, *85*, 1131–1132.
(33) Viani, A.; Cappiello, M.; Pacifici, G. M. Binding of diazepam, salicylic acid, and digitoxin to albumin isolated from fetal and adult serum. *Dev. Pharmacol. Ther.* **1991**, *17*, 100–108.
(34) Wilting, J.; Hart, B. J.; De Gier, J. J. The role of albumin conformation in the binding of diazepam to human serum albumin. *Biochim. Biophys. Acta* **1980**, *626*, 291–298.
(35) Lucas, D.; Menez, J. F.; Daniel, J. Y.; Bardou, L. G.; Floch, H. H. Acetaldehyde adducts with serum proteins: Effect on diazepam and phenytoin binding. *Pharmacology* **1986**, *32*, 134–140.
(36) Kober, A.; Ekman, B.; Sjoholm, I. Direct and indirect determination of binding constants of drug−protein complexes with microparticles. *J. Pharm. Sci.* **1978**, *67*, 107–109.
(37) Muller, W.; Wollert, U. Characterization of the binding of benzodiazepines to human serum albumin. *Naunyn-Schmiedeberg's Arch. Pharmacol.* **1973**, *280*, 229–237.
(38) Chamouard, J. M.; Barre, J.; Urien, S.; Houin, G.; Tillement, J. P. Diclofenac binding to albumin and lipoproteins in human serum. *Biochem. Pharmacol.* **1985**, *34*, 1695–1700.
(39) Epps, D. E.; Raub, T. J.; Kezdy, F. J. A general, wide-rage spectrofluorometric method for measuring the site-specific affinities of drugs toward human serum albumin. *Anal. Biochem.* **1995**, *227*, 342–350.
(40) Zini, R. Les modes de fixation des médicaments sur les proteines plasmatiques humaines et leurs conséquences pharmacologiques. UER de Sciences de l'Université Paris XII, France, Dissertation, 1984.
(41) Tanaka, M.; Asahi, Y.; Masuda, S.; Minagawa, K. Binding position of tolbutamide to human serum albumin. *Chem. Pharm. Bull. (Tokyo)* **1998**, *46*, 817–821.
(42) Judis, J. Binding of sulfonylureas to serum proteins. *J. Pharm. Sci.* **1972**, *61*, 89–93.
(43) Zini, R.; d'Athis, P.; Hoareau, A.; Tillement, J. P. Binding of four sulphonamides to human albumin. *Eur. J. Clin. Pharmacol.* **1976**, *10*, 139–145.
(44) Jakoby, M. G. 4th.; Covey, D. F.; Cistola, D. P. Localization of tolbutamide binding sites on human serum albumin using titration calorimetry and heteronuclear 2-D NMR. *Biochemistry* **1995**, *34*, 8780–8787.
(45) Koizumi, K.; Ikeda, C.; Ito, M.; Suzuki, J.; Kinoshita, T.; Yasukawa, K.; Hanai, T. Influence of glycosylation on the drug binding of human serum albumin. *Biomed. Chromatogr.* **1998**, *12*, 203–210.
(46) Ding, Y.; Zhu, X.; Lin, B. Study of interaction between drug enantiomers and serum albumin by capillary electrophoresis. *Electrophoresis* **1999**, *20*, 1890–1894.

JM7012826